AIP Journal of Applied Physics

Structural phase transformation and phase boundary/stability studies of field-cooled Pb (Mg 1/3 Nb 2/3 O 3) – 32 % Pb Ti O 3 crystals

Hu Cao, Feiming Bai, Jiefang Li, D. Viehland, Guangyong Xu, H. Hiraka, and G. Shirane

Citation: Journal of Applied Physics **97**, 094101 (2005); doi: 10.1063/1.1883723
View online: http://dx.doi.org/10.1063/1.1883723
View Table of Contents: http://scitation.aip.org/content/aip/journal/jap/97/9?ver=pdfcov
Published by the AIP Publishing

Structural phase transformation and phase boundary/stability studies of field-cooled $Pb(Mg_{1/3}Nb_{2/3}O_3)-32\%PbTiO_3$ crystals

Hu Cao,[a] Feiming Bai, Jiefang Li, and D. Viehland
Department of Materials Science and Engineering, Virginia Tech, Blacksburg, Virginia 24061

Guangyong Xu, H. Hiraka,[b] and G. Shirane
Department of Physics, Brookhaven National Laboratory, Upton, New York 11973

(Received 24 January 2005; accepted 9 February 2005; published online 14 April 2005)

Structural phase transformations in (001)-oriented $(1-x)Pb(Mg_{1/3}Nb_{2/3}O_3)-32\%PbTiO_3$ crystals have been investigated by x-ray diffraction. A $C\rightarrow T\rightarrow M_C$ sequence was observed in both the field-cooled and zero-field-cooled conditions. Most interestingly, an anomalous increase in the $C\rightarrow T$ phase boundary with increasing field has been observed, which is seemingly a common characteristic of crystals whose compositions are in the vicinity of the morphotropic phase boundary, irrespective of the width of the T and M_C phase regions. © *2005 American Institute of Physics*. [DOI: 10.1063/1.1883723]

I. INTRODUCTION

Single crystals of the complex perovskite systems $(1-x)Pb(Mg_{1/3}Nb_{2/3}O_3)-xPbTiO_3$ (PMN–x%PT) and $(1-x)Pb(Zn_{1/3}Nb_{2/3}O_3)-xPbTiO_3$ (PZN–x%PT) have exceptional electromechanical properties.[1,2] The ultrahigh piezoelectric constants and field-induced strains—an order of magnitude larger than those of conventional piezoelectric ceramics—have been reported for "*domain-engineered*" (001)-oriented PMN–x%PT and PZN–x%PT crystals for compositions close to a morphotropic phase boundary (MPB). The MPB is supposed to be a near-vertical boundary in the x-temperature (x-T) field, separating rhombohedral (R) and tetragonal (T) phases. For example, in (001)-oriented PMN–x%PT crystals, the composition $x=0.33$ lies at the MPB, and possesses the optimum piezoelectric ($d_{33}\sim 2500\ pC/N$) and electromechanical coupling ($k_{33}\sim 94\%$)[3] coefficients.

Understanding of the structural origin of the high electromechanical properties of MPB compositions has undergone an evolution in thought. Early investigations attributed the high electromechanical properties of $Pb(Zr_{1-x}Ti_x)O_3$ ceramics to domain (or "*extrinsic*" contributions.[4] More recently, coincidental with their discovery of the high electromechanical properties in oriented PMN–x%PT and PZN–x%PT crystals, Park and Shrout[1] conjectured that the ultrahigh strain under applied electric field (E) was due to a $R\rightarrow T$ phase transition induced by E; however, the slim-loop nature of the ε-E curves is not conventional for an induced transition that is generally expected to be strongly hysteretic.

Subsequently, x-ray diffraction (XRD) and neutron diffraction experiments have shown the existence of various monoclinic (M) bridging phases in $PbZr_{(1-x)}Ti_xO_3$ ceramics,[5–7] and in oriented PZN–x%PT[8–12] and PMN–x%PT[12–15] crystals. Two monoclinic phases, M_A and M_C, have since been reported in PZN–x%PT.[8–12] The M_A and M_C notation is adopted following Vanderbilt and Cohen.[16] Recent neutron diffraction studies of the effect of an electric field (E) on PZN–8%PT by Ohwada *et al.*[11] have shown that a cubic $(C)\rightarrow T\rightarrow M_C$ transformational sequence occurs when field cooled (FC), and that a $R\rightarrow M_A\rightarrow M_C\rightarrow T$ sequence takes place with increasing E at 350 K beginning from the zero-field-cooled (ZFC) condition.

Similar M_A and M_C phases have also been reported in PMN–x%PT.[12–15] A recent study by Bai *et al.*[15] established that PMN–30%PT has a $C\rightarrow T\rightarrow M_C\rightarrow M_A$ sequence in the FC condition, and a $R\rightarrow M_A\rightarrow M_C\rightarrow T$ one with increasing E beginning from the ZFC. Optical domain studies also have shown the existence of M phase in PMN–33%PT crystal by Xu *et al.*.[17] Figure 1 summarizes the modified phase diagram of PMN–x%PT in the FC condition; which is re-plotted according to recent data published by Noheda *et al.*[14] and by Bai *et al.*[15] (alongside that to be presented in this article). All black symbols connected by lines represent XRD data taken under $E=0$ kV/cm and all black ones connected by curves represent $E=2$ kV/cm. The polarization vectors of the M_C, T, and R phases within the perovskite unit cell are shown in the inset of this figure. Interestingly, an anomalous shift of T_C towards higher temperatures under electric field (E) was previously reported for PMN–30%PT,[15] as illustrated in this figure. However, it is not yet known if this shift occurs only in a limited phase field in which the transformational sequence in the FC condition is $C\rightarrow T\rightarrow M_C\rightarrow M_A$, where there are limited ranges of T and M_C phase stability; or whether, the increase of the $C\rightarrow T$ boundary with increasing E may be characteristic of a wider phase field, in which the T and M_C phase stability are favored.

In this investigation, we have carefully performed XRD studies to characterize the structure of the composition PMN–32%PT that is located on the PMN-rich side of the MPB as a function of temperature under various electric fields. Here, we report that the shift of the $C\rightarrow T$ phase boundary to higher temperatures with increasing E is a com-

[a]Author to whom correspondence should be addressed; electronic mail: hcao@vt.edu
[b]Permanent address: Institute of Material Research, Tohoku University, Sendai 980-8577, Japan.

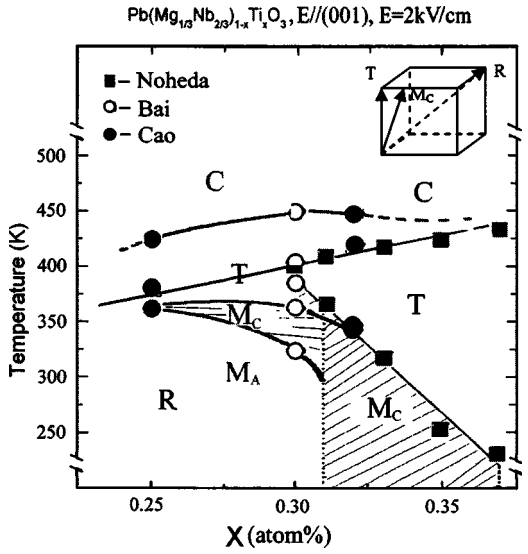

FIG. 1. Modified phase diagram of PMN–xPT around the MPB according to recent data by Noheda *et al.* (see Ref. 14). The solid line indicating the transition to cubic phase is reported by Noblanc *et al.*, black solid squares by Noheda *et al.*, open circles by Bai *et al.* (see Ref. 15), and solid circles by Cao *et al.* in this study. All black signs connected by lines stand for $E=0$ kV/cm and all black ones connected by curves stand for $E=2$ kV/cm. The polarization vectors of monoclinic C (M_C), tetragonal (T) and rhombohedral (R) in the perovskite unit cell are shown as an inset.

mon characteristic of crystals whose compositions are in the vicinity of the MPB, irrespective of the width of the T and M_C phase regions.

II. EXPERIMENTAL PROCEDURE

Crystals of PMN–32%PT with dimension of $3\times3\times3$ mm^3 were obtained from HC Materials (Urbana, IL), and were grown by a top-seeded modified Bridgman method. All surfaces were oriented along (100) pesudocubic faces, and were polished to 0.25 μm. Gold electrodes were deposited on one pair of opposite surfaces of the cube by sputtering—we designate here the electroded faces as (001). Dielectric measurements were performed using a multifrequency *LCR* meter (HP 4284A) to assure that the Curie temperature (T_C) of samples was close to that shown in the phase diagram given by Noheda *et al.*[14] XRD studies were performed using a Philips MPD high-resolution system equipped with a two bounce hybrid monochromator, an open three-circle Eulerian cradle, and a doomed hostage. A Ge (220)-cut crystal was used as an analyzer, which had a θ resolution of 0.0068°. The x-ray wavelength was that of Cu$K\alpha$=1.5406 Å and the x-ray generator was operated at 45 kV and 40 mA. The penetration depth in the samples was on an order of 10 μm. Each measurement cycle was begun by heating up to 550 K to depole the crystal, with measurements taken on decreasing temperature. Measurements made under zero-field cooling are designated as ZFC, whereas those made under field-cooling are designated as FC. At 450 K, the lattice constant of PMN–32%PT was $a=4.027$ Å, correspondingly the reciprocal lattice unit (or 1 rlu) was $a^*=2\pi/a=1.560$ Å^{-1}. All mesh scans of PMN–32%PT shown in this study were plotted in reference to this reciprocal unit.

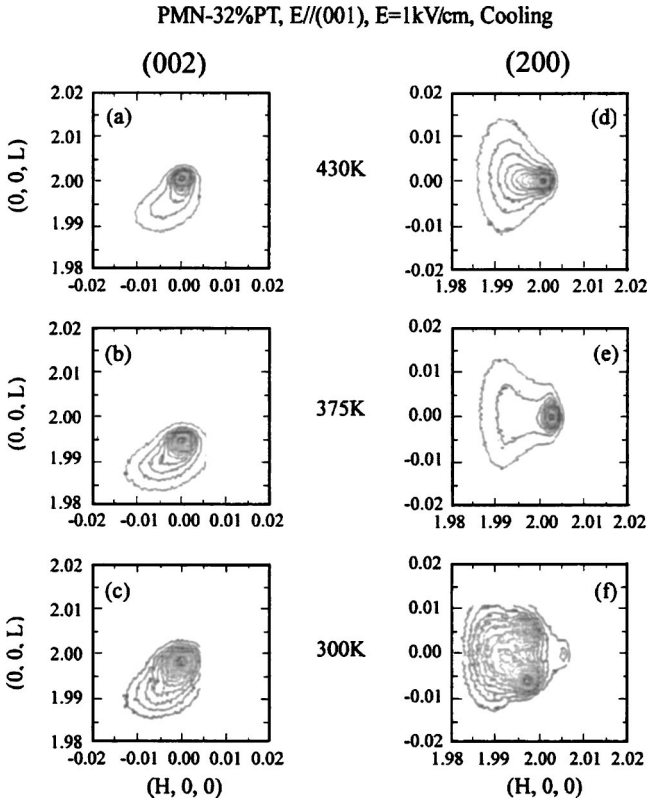

FIG. 2. Mesh scans around the (002) and (200) profiles for PMN–32%PT at 430, 375, and 300 K under as $E=1$ kV/cm on cooling.

III. RESULTS AND DISCUSSION

Figure 2 shows mesh scans taken on cooling under $E=1$ kV/cm. Scans taken at 430 K, which is close to the $C\rightarrow T$ transition, revealed somewhat broadened contours. However, the lattice parameters extracted from these (002) and (200) scans were nearly identical. Possibly, over a narrow temperature range near T_C, there is a small degree of C and T phase coexistence. With decrease of temperature, the (002) peak shifted towards lower L values, and the (200) peak towards higher H values. This demonstrates a $C\rightarrow T$ transition on cooling. However, as shown in the (200) mesh scan at 375 K, an additional weak peak is present, indicating some 90° domain formation along the ⟨101⟩. This is possibly due to the limited penetration depth of our x-ray probe, but either way we did not observe a fully aligned single domain configuration. Upon further cooling to 300 K, the (200) reflection was found to split into three peaks—two (200) peaks, and a single (020) one, whereas the (002) reflection remained as a single peak. Clearly, the (200) and (002) mesh scans at 300 K have the signature features of the M_C phase. The lattice parameters as a function of temperature on cooling under $E=1$ kV/cm are plotted in Fig. 3. At 430 K, a decrease in the a parameter was found at the $C\rightarrow T$ transition. Near the $T\rightarrow M_C$ transition at ~350 K, c_M decreased with respect to c_T, a_M increased with respect to a_T, and b_M was nearly equal to a_T. In general, we found the temperature dependent lattice parameters for PMN–32%PT cooled under $E=1$ kV/cm to be nearly identical to corresponding ones for ceramics in the ZFC condition[14]—both exhibited stable M_C phases at 300 K, with similar values of the lattice parameters.

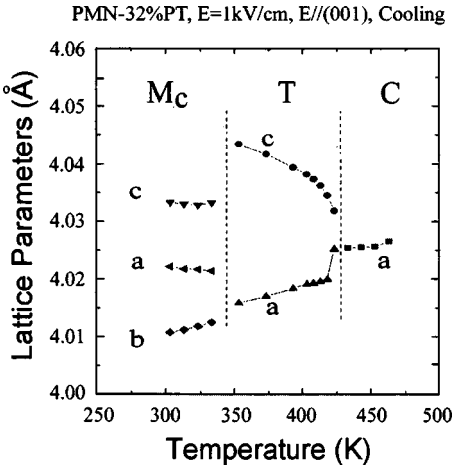

FIG. 3. Evolution of lattice *c* parameters as a function of temperature for PMN–32%PT under $E=1$ kV/cm on cooling.

Figure 4 shows the evolution of (200)-mesh scans of PMN–32%PT with increasing electric field, taken at 300 K in the FC condition. The (200)-mesh scan taken under zero fields is given in Fig. 4(a). A single contour can be seen that is quite broad, possessing a rather long tail that extends along the longitudinal direction. In addition (data not shown), we did not observe any splitting in the (220)-mesh scan, and thus can rule out the possibility that the *R* phase is stable. Figures 4(b) and 4(c) show the (200)-mesh scan under different electric fields. Under a small field of $E=0.5$ kV/cm, the (200)-mesh scan exhibited the signature pattern of the M_C phase; and upon increasing the field to $E=1$ kV/cm, the monoclinic pattern became more pronounced. According to the ZFC phase diagram reported by Noheda *et al.*[14] and redrawn in Fig. 1, PMN–32%PT is located inside of the MPB region, where the monoclinic M_C phase is present at $T=300$ K over the compositional range of $31 \leqslant x \leqslant 37$ at. %. Our results at ZFC did not show the M_C-type splitting, very likely because one or more of the M_C domains were missing, which is quite common in single crystal diffraction measurements. The signature of M_C phase becomes clear with FC, where the field helps stabilize different MC domains. We thus infer that the phase transitional sequence is $C \rightarrow T \rightarrow M_C$ in both the ZFC and FC conditions.

Figure 5(a) shows the dielectric constant as a function of temperature for $350 < T < 460$ K taken under different electric fields in the FC condition. These data were taken on cooling using a measurement frequency of 1 kHz. A single transition can clearly be seen in ZFC condition near 410 K. According to the ZFC phase diagram[14] (redrawn in Fig. 1), this transition is the $C \rightarrow T$ one. Unlike prior results for PMN–30%PT,[15] our dielectric peaks for PMN–32%PT were relatively sharp near T_C, and only weakly frequency dependent (data not shown). In this regard, PMN–32%PT in the ZFC condition exhibits transition characteristics similar to those of a normal ferroelectric, rather than those of a relaxor. However, the $C \rightarrow T$ phase transition temperature, as determined by field dependent dielectric constant measurements, was *not* altered with increasing *E*. Although, in the FC condition, the magnitude of the dielectric constant was dramatically decreased in the *T*-phase region by field cooling, even under a small field of $E=0.5$ kV/cm.

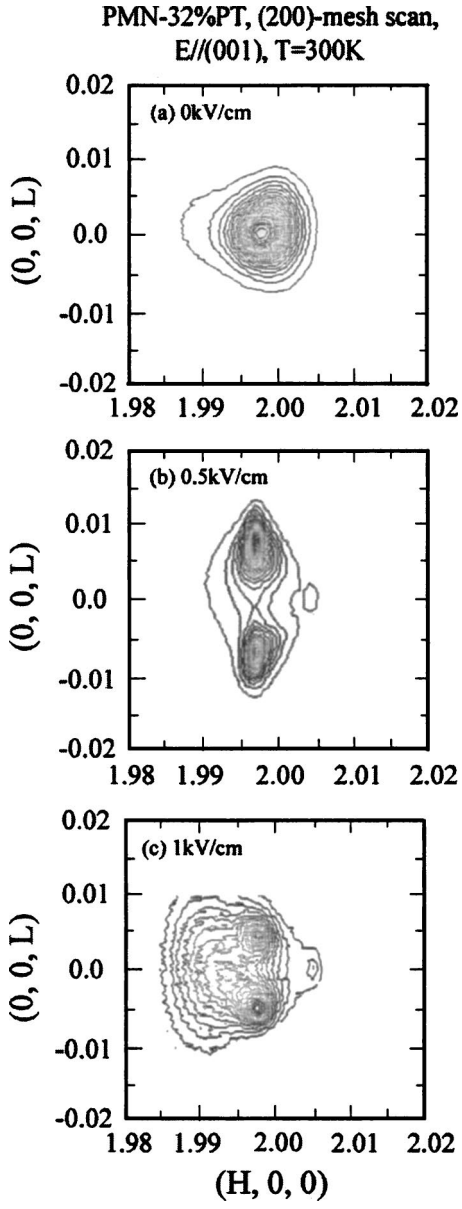

FIG. 4. Electric-field dependence of the (H0L) contour around (200) obtained at 300 K.

Figure 5(b) shows the evolution of the lattice parameter *c* as a function of temperature at different electric fields. Here, we defined T_C as the temperature at which the lattice constant *c* begins to increase in magnitude upon cooling. In this figure, it can clearly be seen that the $C \rightarrow T$ transition shifts towards higher temperature with increasing *E*. We determined the rate of increase in T_C for PMN–32%PT to be ~ 10 K cm/kV. In addition, no abnormal changes in the lattice parameter values or its slope can be seen in Fig. 5(b) for temperatures below 410 K. This indicates that there is a region where the *T* and *C* phases coexist, which is also consistent with our above observations in Fig. 2 concerning the mesh scans at 430 K.

An important observation from this work for PMN–32%PT is an apparent difference between T_C as determined by comparisons of dielectric and structural measurements in

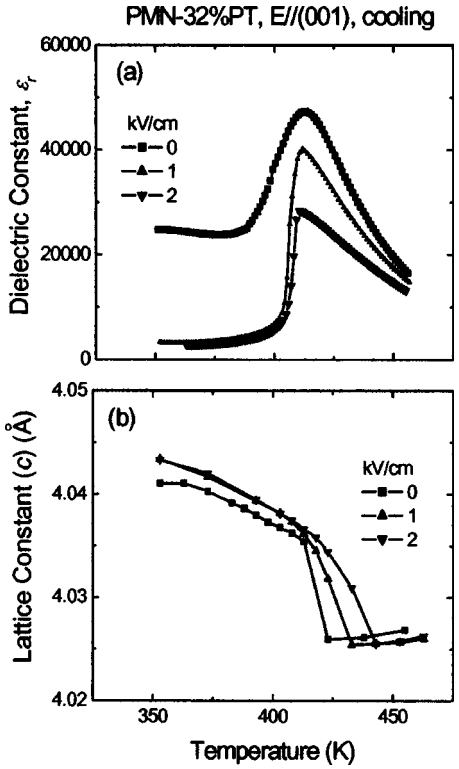

FIG. 5. Temperature dependence of (a) the dielectric constants at 1 KHz and (b) lattice constants derived from (002) reflection under different levels of electric fields.

the FC condition. We summarize in the PMN–x%PT phase diagram of Fig. 1 the shift in the $C \rightarrow T$ boundary upon application of $E=2$ kV/cm (shown as curve), as determined by XRD. The corresponding $C \rightarrow T$ boundary, determined from dielectric measurements taken under $E=2$ kV/cm, follow that of the ZFC condition (shown as line). Also summarized in this figure is the relative magnitude of the shift in the $C \rightarrow T$ phase boundary over a wide composition field (note: all XRD data). It is relevant to notice that the $C \rightarrow T$ boundary shift rate was reduced as the MPB was approached, with increasing x. For example, we observed a shift rate of $\delta T_c / \delta E \sim 10$ K cm/kV for PMN–32%PT, whereas the shift rate for PMN–32%PT was previously reported to be ~ 25 K cm/kV.[15] Furthermore, in this investigation, we found PMN–25%PT (which has relaxor characteristics) to have an identical rate to that for PMN–30%PT with $\delta T_c / \delta E \sim 25$ K cm/kV (data not shown, but summarized in the phase diagram). Our summary of results demonstrates that the increase of the $C \rightarrow T$ boundary with increasing E is not limited to a phase field with narrow ranges of T and M_C stability, but rather is seemingly a common characteristic of crystals whose compositions are in the vicinity of the left-hand side of the MPB, irrespective of the width of the T and M_C phase regions. Although, the value of $\delta T_c / \delta E$ is reduced as one approaches the MPB, and crosses over into the T-phase region on the right-hand side of the MPB.

One possible explanation for the dependence of the $C \rightarrow T$ phase boundary on E is that polar nanodomains (PND) exists near T_C, for compositions on the left-hand side of the MPB. Application of E along (001) might then readily favor an alignment of PND whose polarization is oriented along the c axis. The observed shift in the $C \rightarrow T$ phase boundary could then simply reflect a change in the relative population of tetragonal PND variants under E. Due to the diffuse nature of the transition, the volume fraction of tetragonal PND would gradually increase on cooling over a relatively broad temperature range, allowing for gradual lattice parameter changes. However, for PMN–32%PT whose c/a ratio is larger in the T phase than PMN–30%PT, the coexistence of tetragonal domains with the cubic phase would be suppressed by a significantly higher elastic energy density, i.e., $\sim (c/a)^2$. Thus, the $C \rightarrow T$ phase transformation near and above the MPB would be sharper, and its phase boundary more difficult to shift under E.

In summary, structural and dielectric measurements of (001)-oriented PMN–32%PT crystals have been performed. A $C \rightarrow T \rightarrow M_C$ sequence was found in both the ZFC and FC conditions. However, an important change was observed in the structural data with increasing E—an anomalous increase in the $C \rightarrow T$ boundary with increasing E was found, which becomes less pronounced on approaching the MPB.

ACKNOWLEDGMENTS

The authors would like to gratefully acknowledge financial support from the U.S. Department of Energy under Contract No. DE.-AC02-98CH10886 and the Office of Naval Research under Grant Nos. N000140210340, N000140210126, and MURI N0000140110761. The authors would also like to thank H. C. Materias for providing the single crystals used in this study.

[1] S.-E. Park and T. R. Shrout, J. Appl. Phys. **82**, 1804 (1997).
[2] S. F. Liu, S.-E. Park, T. R. Shrout, and L. E. Cross, J. Appl. Phys. **85**, 2810 (1999).
[3] H. S. Luo, G. S. Xu, H. Q. Xu, P. C. Wang, and Z. W. Yin, Jpn. J. Appl. Phys., Part 1 **39**, 5581 (2000).
[4] C. Randall, M. Kim, J. Kucera, W. Cao, and T. Shrout, J. Am. Ceram. Soc. **81**, 677 (1998).
[5] B. Noheda, D. E. Cox, G. Shirane, J. A. Gonzalo, L. E. Cross, and S.-E. Park, Appl. Phys. Lett. **74**, 2059 (1999).
[6] B. Noheda, J. A. Gonzalo, L. E. Cross, R. Guo, S.-E. Park, D. E. Cox, and G. Shirane, Phys. Rev. B **61**, 8687 (2000).
[7] B. Noheda, D. E. Cox, G. Shirane, R. Guo, B. Jones, and L. E. Cross, Phys. Rev. B **63**, 014103 (2000).
[8] B. Noheda, D. E. Cox, G. Shirane, S. E. Park, L. E. Cross, and Z. Zhong, Phys. Rev. Lett. **86**, 3891 (2001).
[9] D. La-Orauttapong, B. Noheda, Z. G. Ye, P. M. Ghering, J. Toulouse, D. E. Cox, and G. Shirane, Phys. Rev. B **65**, 144101 (2002).
[10] B. Noheda, Z. Zhong, D. E. Cox, G. Shirane, S. E. Park, and P. Rehrig, Phys. Rev. B **65**, 224101 (2002).
[11] K. Ohwada, K. Hirota, P. Rehrig, Y. Fujii, and G. Shirane, Phys. Rev. B **67**, 094111 (2003).
[12] J. Kiat, Y. Uesu, B. Dkhil, M. Matsuda, C. Malibert, and G. Calvarin, Phys. Rev. B **65**, 064106 (2002).
[13] Z. G. Ye, B. Noheda, M. Dong, D. Cox, and G. Shirane, Phys. Rev. B **64**, 184114 (2001).
[14] B. Noheda, D. E. Cox, G. Shirane, J. Gao, and Z. G. Ye, Phys. Rev. B **66**, 054104 (2002).
[15] F. Bai, N. Wang, J. Li, D. Viehland, P. Gehring, G. Xu, and G. Shirane, J. Appl. Phys. **96**, 1620 (2004).
[16] D. Vanderbilt and M. Cohen, Phys. Rev. B **63**, 094108 (2001).
[17] G. Xu, H. Luo, H. Xu, and Z. Yin, Phys. Rev. B **64**, 020102 (2001).